Molecular reorientations of bicyclo [2, 2, 2] octane in its plastic solid phase : correlation times from incoherent quasielastic neutron scattering study

M. Bée, J.L. Sauvajol, J.P. Amoureux

▶ **To cite this version:**

M. Bée, J.L. Sauvajol, J.P. Amoureux. Molecular reorientations of bicyclo [2, 2, 2] octane in its plastic solid phase : correlation times from incoherent quasielastic neutron scattering study. Journal de Physique, 1982, 43 (12), pp.1797-1808. 10.1051/jphys:0198200430120179700 . jpa-00209563

HAL Id: jpa-00209563
https://hal.science/jpa-00209563v1

Submitted on 4 Feb 2008

HAL is a multi-disciplinary open access archive for the deposit and dissemination of scientific research documents, whether they are published or not. The documents may come from teaching and research institutions in France or abroad, or from public or private research centers.

L'archive ouverte pluridisciplinaire **HAL**, est destinée au dépôt et à la diffusion de documents scientifiques de niveau recherche, publiés ou non, émanant des établissements d'enseignement et de recherche français ou étrangers, des laboratoires publics ou privés.

Classification
Physics Abstracts
61.50E — 61.50K — 61.12 — 64.70K

Molecular reorientations of bicyclo [2, 2, 2] octane in its plastic solid phase : correlation times from incoherent quasielastic neutron scattering study

M. Bée (*+), J. L. Sauvajol (+) and J. P. Amoureux (+)

(*) Institut Laue-Langevin, 156X, Centre de Tri, 38042 Grenoble Cedex, France
(+) Laboratoire de Dynamique des Cristaux Moléculaires (**),
Université des Sciences et des Techniques de Lille, 59655 Villeneuve d'Ascq Cedex, France

(*Reçu le 17 mai 1982, révisé le 10 août, accepté le 27 août 1982*)

Résumé. — La diffusion quasi élastique incohérente des neutrons a permis d'étudier les réorientations moléculaires du bicyclo [2, 2, 2] octane $CH(CH_2CH_2)_3CH$ dans sa phase plastique. Les mesures ont été effectuées dans un domaine de température allant de 173 K à 359 K, pour quatre valeurs de la longueur d'onde des neutrons incidents, en utilisant un échantillon polycristallin. L'allure des spectres quasi élastiques observés est décrite par un modèle dans lequel les molécules effectuent des sauts réorientationels entre six positions d'équilibre également espacées de 60° autour de l'axe de symétrie, avec en outre un basculement de la molécule d'une direction [111] du réseau cristallin à une autre équivalente. Les valeurs finales des temps de corrélation obéissent aux deux lois d'Arrhénius :

$$\tau_{M_6} = 1{,}743 \times 10^{-13} \exp(\Delta H_M/RT)\ \text{s} \qquad \Delta H_M = 5{,}64\ \text{kJ/mole}$$
$$\tau_{C_4} = 1{,}952 \times 10^{-13} \exp(\Delta H_C/RT)\ \text{s} \qquad \Delta H_C = 8{,}90\ \text{kJ/mole}\,.$$

Aux températures les plus élevées, une description sur la base d'un modèle de diffusion rotationnelle est aussi examinée.

Abstract. — Using the incoherent quasielastic neutron scattering technique, we have studied the molecular reorientations of bicyclo [2, 2, 2] octane $CH(CH_2CH_2)_3CH$ in its plastic phase. A sample temperature ranging from 173 K to 359 K was used with four values of incoming neutron wavelength, using a polycrystalline sample. The observed quasielastic spectra are described by a model in which the molecules perform reorientational jumps between six equilibrium positions equally spaced by 60° around the molecular symmetry axis, together with a tumbling of the molecule from a [111] lattice direction to an equivalent position. The resulting values of the correlation times follow the two Arrhénius laws :

$$\tau_{M_6} = 1.743 \times 10^{-13} \exp(\Delta H_M/RT)\ \text{s} \qquad \Delta H_M = 5.64\ \text{kJ/mole}$$
$$\tau_{C_4} = 1.952 \times 10^{-13} \exp(\Delta H_C/RT)\ \text{s} \qquad \Delta H_C = 8.90\ \text{kJ/mole}\,.$$

For the highest temperatures, a description on the basis of the rotational diffusion model is also examined.

1. **Introduction.** — In the study of translational and rotational degrees of freedom of condensed molecular phases, four main classes are usually distinguished. Isotropic liquids exhibit a translational and rotational disorder, whilst liquid crystals are orientationally ordered but translationally disordered. Plastic crystals are orientationally disordered crystals with translational order but in brittle crystals both translational and rotational degrees of freedom are ordered [1]. We are concerned with the orientationally-disordered phases. These phases are characteristic of crystals consisting of globular or highly symmetrical molecules such as adamantane (and derivatives), methane, etc... Molecules with internal degrees of freedom, such as succinonitrile or pivalic acid (where methyl groups, whole t-butyl group or carboxylic group are enabled to rotate), also exhibit a plastic phase over a wide temperature range. With decreasing the temperature, order is usually achieved in several stages : several orientational phase transitions may be observed with a stepwise reduction of the orientational disorder.

(**) ERA 465.

Article published online by EDP Sciences and available at http://dx.doi.org/10.1051/jphys:0198200430120179700

Structural, thermodynamic and motional properties of molecular crystals may be understood semi-quantitatively by use of intermolecular potentials. These weak non-isotropic interactions mainly originate from the weak Van der Waals forces, reflecting both the symmetry of the molecule and that of its surrounding. The radial part of the potential is responsible for the translational order, whilst the angle-dependent part of the potential governs the orientational ordering of the molecules. The minima of this potential generally determine several equilibrium positions. Different cases are possible, according to the height of the barriers of the potential and the temperature. If the temperature is sufficiently low, the angular average of the intermolecular forces is much stronger than the fluctuating contribution arising from the thermal motions. The molecules either do not reorient at all, or perform only occasional orientational jumps, dictated by their own symmetry operations. In most cases, when the temperature is increased, a phase transition occurs, in which the equilibrium positions of the centres of mass of the molecules are changed. Reorientational jumps between new, distinguishable, equilibrium orientations lead to an apparent (statistical) increase in the symmetry of the crystal.

Our aim was to study the nature of the molecular motion in such a plastic phase, namely that of bicyclo [2, 2, 2] octane $CH(CH_2\underline{CH}_2)_3CH$. It is a globular, cage-like molecule with $\bar{6}m2$ symmetry (Fig. 1). This compound undergoes a solid-solid phase transition at 164.25 K and melts at 447.48 K [2]. The associated entropy increments, $\Delta S_t = 6.66$ cal./mol. K and $\Delta S_m = 4.48$ cal./mol. K, are positive evidence of the plastic nature of this high-temperature solid phase. Below 164.25 K, an X-ray powder diffraction study has established that the structure of the low-temperature phase is hexagonal [3]. The determination of the crystalline structure of the high-temperature phase [4] (Fm3m, $Z = 4$) confirms the existence of an orientational disorder. In the present paper we wish to report incoherent quasielastic neutron scattering (IQNS) results. The plastic phase of another similar compound, quinuclidine, has been studied previously by X-ray [5], NMR [6] and IQNS [7]. Using the neutron technique, we have also investigated both the low- and the high-temperature phases of triethylene diamine. We shall report on these results elsewhere.

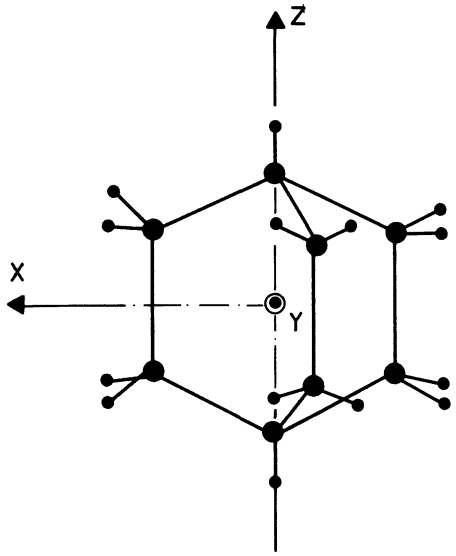

Fig. 1. — The bicyclo [2, 2, 2] octane molecule.

2. **The scattering law and the models.** — The refinement of the crystalline structure using symmetry-adapted functions [4] shows that the maximum of the orientational probability occurs when the threefold molecular and crystal axes are coincident. We have already demonstrated [19] that the sign and the amplitude of the coefficients $A^l_{mm'}$ in the expansion of the orientational probability of the molecule $f(\omega)$ on the basis of the rotator functions $R^l_{mm'}(\omega)$ (ω are the usual Euler angles)

$$f(\omega) = \sum_{lmm'} \frac{(2\,l+1)}{8\,\pi^2} A^l_{mm'}\, R^l_{mm'}(\omega) \qquad (1)$$

show the importance of the molecular delocalization. In the case of bicyclo-octane the value of A^4_{11} was found to be $-\,0.382 \pm 0.24$, which is to be compared with 0.763 if the molecular threefold axis were *fixed* along [111]. Moreover, the small values of other coefficients, such as A^6_{13}, A^8_{13}, suggest a quasi-uniform rotation of the molecule about the molecular threefold axis. These results of the high-temperature crystalline structure analysis will be helpful for building models to describe the molecular motions.

2.1 ISOTROPIC ROTATIONAL DIFFUSION MODEL. — Let us consider first the so-called isotropic rotational diffusion model, in which the molecules are assumed to perform more-or-less continuous small-angle random rotations. Thus, on a time-average, they have no preferred orientation in space. For bicyclo-octane, at room temperature, this is in conflict with the X-ray results. Nevertheless, its introduction is worthwhile for the analysis of the measurements at the higher temperatures.

This model is well-known [8] and under the assumptions above, the rotational incoherent scattering function for one proton moving on a sphere of radius r can be written

$$S(Q,\omega) = A_0(Q)\,\delta(\omega) + \sum_{l=1}^{\infty} A_l(Q) \cdot \frac{1}{\pi} \cdot \frac{\tau_l}{1+\omega^2\,\tau_l^2}. \qquad (2)$$

The elastic and quasielastic structure factors are functions of the Bessel spherical functions $j_l(Qr)$

$$A_0(Q) = j_0^2(Qr) \qquad (3a)$$

$$A_l(Q) = (2\,l+1)\,j_l^2(Qr) \qquad (3b)$$

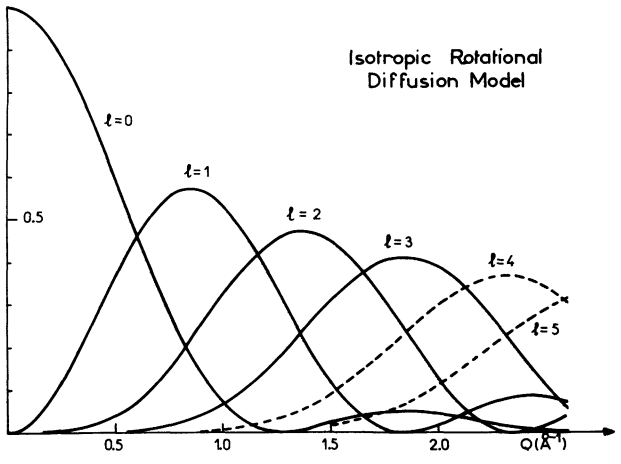

Fig. 2. — Elastic and quasielastic structure factors for the isotropic rotational diffusion model (Eq. (3)).

τ_l is the correlation time for the spherical harmonic of order l

$$\tau_l^{-1} = l(l + 1)\, D_R \qquad (4)$$

D_R, the isotropic diffusion constant is the only adjustable parameter. In the bicyclo-octane, there are two types of hydrogen atoms, which move on separate shells. Firstly these are 12 hydrogen atoms bonded to a secondary carbon, which move on a sphere of radius $R_S = 2.45$ Å and secondly 2 hydrogen atoms bonded to a tertiary carbon, moving on a sphere of radius $R_T = 2.26$ Å. Figure 2 shows the elastic and quasielastic structure factors, calculated on the basis of (3) and averaged over the two types of protons. It is evident that the infinite sum occurring in (2) can be truncated at a small l value (namely $l = 5$ for the measurements using the time focusing time-of-flight spectrometer IN6 and $l = 4$ when using the four chopper time-of-flight spectrometer IN5). This model can only be valid if the potential in which the molecule rotates is weak, or if the sample-temperature is high. Generally this is not the case and the molecular motion is more commonly described on the basis of instantaneous reorientational jump models.

2.2 Reorientational jump models. — When the temperature is comparable with the potential barriers, the jump model of Frenkel is usually used [9]. This model assumes a set of preferential orientations for the molecules around which they oscillate. From thermal activation, reorientations of the molecules occur between these orientations. The jumps are assumed to be instantaneous and one does not seek to describe the motion of the molecule when passing from one orientation to another. In spite of the fact that this assumption is strictly not true, the number of molecules performing a reorientation is much less than the number of molecules in the minima. Consequently, accepting that the real motion is much more complicated, in most cases until now, it has been possible to give an adequate description of the motions on the basis of jump-models with a set of discrete orientations located on the minima of the continuous orientational distribution function.

The X-ray study mentioned above suggests the existence of two kinds of molecular motions, a rotation of the molecule around its threefold axis, and also reorientational jumps which bring this axis from one [111] direction of the lattice to another. However, it is conceivable that the corresponding correlation times may differ sufficiently from each other that one of them would arise outside the instrument energy range. Generally, uniaxial rotation is the last motion which subsists as the temperature decreases. In the case of bicyclo-octane, the X-ray crystalline structure result enables us to consider the above assumption to be sufficiently realistic. Thus we should take into account first the rotation of the molecule around its own symmetry axis alone. The disorder of this axis between the [111] lattice directions will be considered to be static.

2.2.1 *Reorientations about molecular axis.* — Two distinguishable orientations are available to the molecule around its axis [4]. Taking into account the molecular symmetry, each of the 12 hydrogens bonded to a secondary carbon performs reorientational jumps on a circle of radius $r_S = 2.15$ Å between six positions equally spaced by 60°. The 2 hydrogens bonded to a tertiary carbon are fixed on the rotation axis. For a polycrystalline sample, the rotational scattering function for the whole molecule can be written [10, 11] :

$$S^R_{inc}(Q, \omega) = a_0(Q)\, \delta(\omega) + \frac{1}{\pi} \sum_{l=1}^{5} a_l(Q) \frac{\tau_l}{1 + \omega^2 \tau_l^2} \qquad (5)$$

with

$$a_0(Q) = \frac{1}{7}\left[1 + \sum_{j=1}^{6} j_0\left(2\, Q r_S \sin \frac{\pi_j}{6}\right)\right] \qquad (6a)$$

and

$$a_l(Q) = \frac{1}{7} \sum_{j=1}^{6} j_0\left(2\, Q r_S \sin \frac{\pi_j}{6}\right) \cos\left(\frac{2\pi l_j}{6}\right). \qquad (6b)$$

The half-widths at half maximum τ_l^{-1} of the Lorentzian functions are defined as :

$$\tau_l^{-1} = \frac{2}{\tau} \sin^2 \frac{\pi l}{6}. \qquad (7)$$

The residence time, τ, is the mean-time spent between two successive jumps of the proton. Equation (7) above assumes that only $\pi/3$ rotations occur. Taking into account the possible existence of $2\pi/3$ and π rotations would require the use of group theory [12, 13]. In fact, the characters of the different M_η ($M_\eta = 2\pi\eta/6$, $\eta = 1, 2, ..., 6$) rotations in the irreducible representation Γ_μ ($\mu = 1, 2, ..., 6$) of the group C^6 can be expressed as :

$$\chi^\eta_\mu = \exp\left(i \frac{2\pi\eta\mu}{6}\right). \qquad (8)$$

Table I. — *Widths of the Lorentzian functions and expression of the elastic* (EISF) *and quasielastic structure factors. The terms $a_l(Q)$ can be calculated from* (6*a*) *and* (6*b*). *The value $\tau_0^{-1} = 0$ corresponding to purely elastic scattering has been added to the others calculated from* (7). *This would correspond in equation* (7) *to the case $l=0$ or $l = 6$ i.e. to the case where the proton remains fixed or undergoes a jump returning it back into its original position.*

$\frac{1}{\tau} = 0$	$A_0(Q) = a_0(Q) = \frac{1}{7}[2 + 2j_0(QR_S) + 2j_0(QR_S\sqrt{3}) + j_0(2QR_S)]$
$\frac{1}{\tau_1} = \frac{1}{\tau_5} = \frac{0.5}{\tau}$	$A_1(Q) = a_1(Q) + a_5(Q) = \frac{1}{7}[2 + 2j_0(QR_S) - 2j_0(QR_S\sqrt{3}) - 2j_0(2QR_S)]$
$\frac{1}{\tau_2} = \frac{1}{\tau_4} = \frac{1.5}{\tau}$	$A_2(Q) = a_2(Q) + a_4(Q) = \frac{1}{7}[2 - 2j_0(QR_S) - 2j_0(QR_S\sqrt{3}) + 2j_0(2QR_S)]$
$\frac{1}{\tau_3} = \frac{2}{\tau}$	$A_3(Q) = a_3(Q) = \frac{1}{7}[1 - 2j_0(QR_S) + 2j_0(QR_S\sqrt{3}) - j_0(2QR_S)]$

Since a rotation of $+\alpha$ (with $\alpha = \pi/3, \pi/2, ...$) has an equal probability to occur that a rotation of $-\alpha$, we obtain for the correlation times τ_μ related to each irreducible representation :

$$\frac{1}{\tau_\mu} = \frac{4}{\tau_{60}} \sin^2 \frac{\pi\mu}{6} + \frac{4}{\tau_{120}} \sin^2 \frac{\pi\mu}{3} + \frac{2}{\tau_{180}} \sin^2 \frac{\pi\mu}{2} \quad (9)$$

in which τ_{60} (resp. τ_{120}, τ_{180}) denotes the mean residence time between two successive $+60°$ (resp. $+120°$, $+180°$) jumps which is equal to the mean residence time between two successive $-60°$ (resp. $-120°$, $-180°$) jumps. With the further assumption that only $\pi/3$ rotations occur, we obtain

$$\frac{1}{\tau_\mu} = \frac{4}{\tau_{60}} \sin^2 \frac{\pi\mu}{6}. \quad (10)$$

This expression is quite analogous to (7). Indeed, in (7), τ, is the mean residence time between two successive jumps of 60° but without any consideration of sense of direction ($+60°$ or $-60°$). Obviously we have

$$\tau_{60} = 2\tau. \quad (11)$$

The Lorentzian widths, as calculated from (7) above, are reported in table I. It can be seen that only four of them are different. The particular value $\tau_0^{-1} = 0$ corresponding to purely elastic scattering has also been reported. Adding together the coefficients $a_l(Q)$ related to the same value of τ_l^{-1}, the rotational scattering law now takes the form :

$$S^R_{inc}(Q, \omega) = A_0(Q)\,\delta(\omega) + \sum_{l=1}^{3} A_l(Q) \cdot \frac{1}{\pi} \cdot \frac{\tau_l}{1 + \omega^2 \tau_l^2}. \quad (12)$$

The expressions for the coefficients $A_l(Q)$ are reported in table I. Figure 3 shows their respective variations as a function of the modulus of the scattering vector Q.

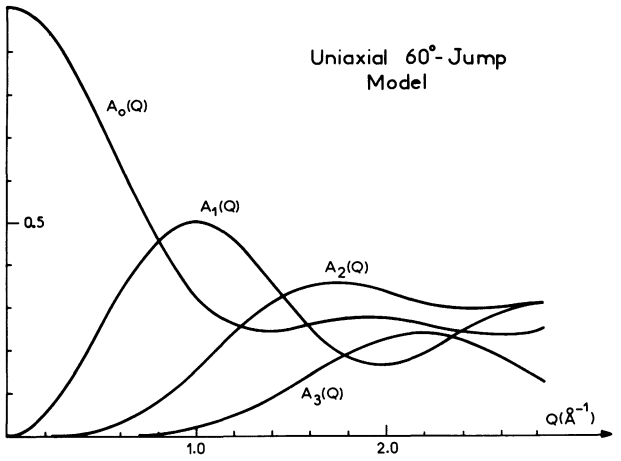

Fig. 3. — Elastic and quasielastic structure factors for the uniaxial 60° jump model (Table I).

As we have already mentioned, the X-ray study has shown that it would be possible to describe the incoherent rotational scattering law for one proton by the expression [10, 15]

$$S^R_{inc}(\mathbf{Q}, \omega) = J_0^2(Qr_S \sin\beta)\,\delta(\omega) + 2\sum_{l=1}^{\infty} J_l^2(Qr_S \sin\beta) \frac{1}{\pi} \frac{l^2 D_r}{l^4 D_r^2 + \omega^2} \quad (13)$$

where J_l is a Bessel function of the first kind and D_r the rotational diffusion constant (uniaxial), and β denotes the angle between the scattering vector and the rotation axis. In the case of powder the equation (13) above has to be averaged over all possible values of β. Unfortunately, no analytical expression can be given. In fact, with a number of jumps $\geqslant 6$, equations (12) and (13) lead to practically the same results [10, 15] for the two cases, at least while $Qr_S \leqslant \pi$ (i.e. in our case $Q \leqslant 1.28$ Å^{-1}, which is just the largest Q value which can be accessed with IN5 when using an incident wavelength $\lambda = 9$ Å). The Q range beyond 1.28 Å^{-1}, where the differences are noti-

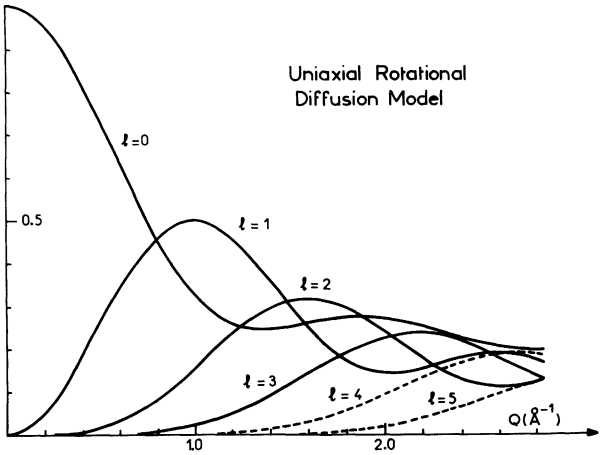

Fig. 4. — Elastic and quasielastic structure factors for the uniaxial rotational diffusion model (Eq. (13)).

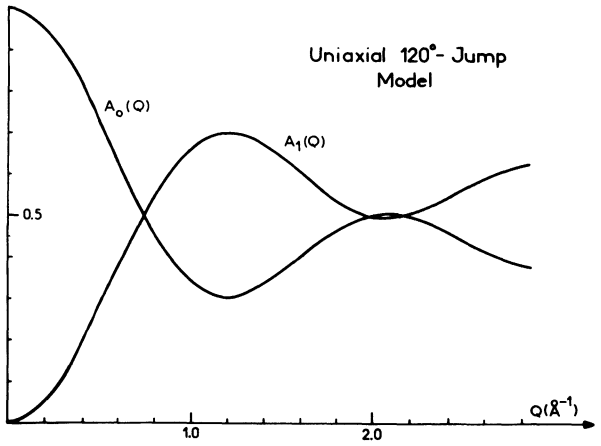

Fig. 5. — Elastic and quasielastic structure factors for the uniaxial 120° jump model (Eq. (15)).

ceable (see Fig. 4) can be reached when using a shorter incident wavelength. However, the instrument resolution is somewhat inferior (even using IN6). Moreover these models are most likely to be valid only at lowest temperatures, where the quasielastic broadening of the spectra is small. Then the distinction between the two models would not be easy.

Table II shows a comparison of the widths of the Lorentzian functions for both models. It can be seen that the ratio of the first correlation times do not coincide in both models. Moreover, the jump model is restricted to $l \leqslant 3$. But at lower Q values, the main contribution to the quasielastic scattering arises from $1/\tau_1$ (refer to $A_1(Q)$ value in figures 3 and 4) and it is impossible to distinguish unambiguously between the two models. Usually, the rotational diffusion constant D_r can be identified with the jump rate probability $1/\tau_1$ given by (7)

$$D_r \simeq \frac{1}{\tau_1} = \frac{2}{\tau} \sin^2 \frac{\pi}{6}. \qquad (14)$$

Table II. — *Comparison of the widths of the Lorentzian functions for a rotational diffusion model and a jump model between six equilibrium positions equally spaced on a circle. Symbols are defined in the text.*

		Jump model	
l	$l^2 D_r$	$\frac{1}{\tau_l}$	$\frac{\tau_1}{\tau_l}$
0	0	0	0
1	D_R	$\frac{1}{\tau_1} = \frac{0.5}{\tau}$	1
2	$4 D_R$	$\frac{1.5}{\tau}$	3
3	$9 D_R$	$\frac{2}{\tau}$	4
4	$16 D_R$		

The low-temperature phase is hexagonal [3] and the dynamical molecular disorder, if it exists, has to be analysed in terms of 120° jumps about the threefold symmetry axis of the molecule. The corresponding rotational incoherent scattering law is (for the whole molecule)

$$S^R_{inc}(Q, \omega) = \frac{1}{7}(3 + 4 j_0(Q r_S \sqrt{3}))\, \delta(\omega) + \frac{4}{7}(1 - j_0(Q r_S \sqrt{3}))\, \frac{1}{\pi} \cdot \frac{\tau'}{1 + \omega^2 \tau'^2} \qquad (15)$$

with the correlation time

$$\tau' = \frac{2}{3}\tau. \qquad (16)$$

The variations of the elastic and quasielastic structure factors are shown in figure 5.

2.2.2 *Reorientations about molecular and crystalline axes.* — The method indicated by G. Rigny [12], C. Thibaudier and F. Volino [13, 14] to calculate the scattering function when motions about both fixed (crystallographic) and mobile (molecular) axes are involved, is now well-known. Under the assumption that the two kinds of rotations are uncorrelated, i.e. that the probability per unit time of any reorientation of the molecule is independent of its precise equilibrium orientation, the application of group theory permits us to calculate both the relevant correlation times and the corresponding elastic and quasielastic structure factors. As bicyclo-octane is almost globular in shape, its inertia tensor is nearly isotropic :

$$(I_3 - I_1)/I_3 \simeq 0.07.$$

The probability of a rotation about any crystallographic axis can be considered as completely independent of the direction along which the molecular symmetry axis is lying.

According to references [12-14] the correlation times are given by the relation :

$$\frac{1}{\tau_\mu} = \sum_\nu \frac{1}{\tau_\nu}\left(1 - \frac{\chi_\mu^{\nu e}}{\chi_\mu^{Ee}}\right) + \sum_\eta \frac{1}{\tau_\eta}\left(1 - \frac{\chi_\mu^{E\eta}}{\chi_\mu^{Ee}}\right) \quad (17)$$

$\chi_\mu^{\nu\eta}$ is the character of the product of the crystalline and the molecular M_η rotations in the irreducible representation Γ_μ of the group product $0 \times C^6$, which is the direct product

$$\Gamma_\mu = \Gamma_{\mu_c} \otimes \Gamma_{\mu_m} \quad (18a)$$

of the two irreducible representations of the crystalline group Γ_{μ_c} and of the molecular group Γ_{μ_m}. These characters are the products

$$\chi_\mu^{\nu\eta} = \chi_\mu^\nu \cdot \chi_\mu^\eta . \quad (18b)$$

The indexes E and e refer, respectively, to the identical operation of the crystalline and molecular group. Evaluation of the correlation times from (17) is straightforward. However, the resulting expressions involve a large number of parameters namely the correlation times related to each rotation of both 0 and C groups. As it seems *a priori* difficult to get them all, a further assumption is needed. We shall assume that reorientations around the molecular axis comprise only $\pm$ 60° jumps from one equilibrium position to a neighbouring one. For the rotations about crystalline axes, we suppose that only rotations which are strictly equivalent in their class have a non-vanishing probability. These are 90° jumps about any of the [100] directions. It follows that we are led to 20 correlation times depending only on the two parameters τ_{C_4} and τ_{M_6} (see Table III).

The elastic and quasielastic structure factors can be calculated from the general relation

$$a_\mu(Q) = \frac{\chi^{Ee}}{g} \sum_\nu \sum_\eta \chi_\mu^{\nu\eta} \sum_{C_\nu} \sum_{M_\eta} j_0(Q \mid \mathbf{r} - C_\nu M_\eta \mathbf{r} \mid) . \quad (19)$$

The sums over ν and η run over all the classes of the crystalline group and of the molecular group, respectively. The two others correspond to summations over all the rotations, C_ν, of the crystalline class, ν, and over all the rotations, M_η, of the molecular class, η. The order of the group product is g. In this expression, the polycrystalline nature of the sample has been taken into account and the average over all directions of **Q** has been performed. Expression (20) has to be calculated for each of the two types of hydrogen and a weighted average must be taken. After a somewhat tedious calculation, analytical expressions for the 20 structure factors were obtained. These involve a large number of jump distances. For our purpose, it is not necessary to give these exact expressions here. They were checked from a numerical calculation, using the

Table III. — *Correlation times for the jump model allowing for crystalline* C_4 *(i.e.* 90°*) and molecular* M_6 *(i.e.* 60°*) jumps.*

$$\begin{aligned}
1/\tau_1 &= 0 \\
1/\tau_2 &= 2/\tau_{M_6} \\
1/\tau_3 &= 1/2\ \tau_{M_6} \\
1/\tau_4 &= 3/2\ \tau_{M_6} \\
1/\tau_5 &= 2/\tau_{C_4} \\
1/\tau_6 &= 2/\tau_{C_4} + 2/\tau_{M_6} \\
1/\tau_7 &= 2/\tau_{C_4} + 1/2\ \tau_{M_6} \\
1/\tau_8 &= 2/\tau_{C_4} + 3/2\ \tau_{M_6} \\
1/\tau_9 &= 1/\tau_{C_4} \\
1/\tau_{10} &= 1/\tau_{C_4} + 2/\tau_{M_6} \\
1/\tau_{11} &= 1/\tau_{C_4} + 1/2\ \tau_{M_6} \\
1/\tau_{12} &= 1/\tau_{C_4} + 3/2\ \tau_{M_6} \\
1/\tau_{13} &= 4/3\ \tau_{C_4} \\
1/\tau_{14} &= 4/3\ \tau_{C_4} + 2/\tau_{M_6} \\
1/\tau_{15} &= 4/3\ \tau_{C_4} + 1/2\ \tau_{M_6} \\
1/\tau_{16} &= 4/3\ \tau_{C_4} + 3/2\ \tau_{M_6} \\
1/\tau_{17} &= 2/3\ \tau_{C_4} \\
1/\tau_{18} &= 2/3\ \tau_{C_4} + 2/\tau_{M_6} \\
1/\tau_{19} &= 2/3\ \tau_{C_4} + 1/2\ \tau_{M_6} \\
1/\tau_{20} &= 2/3\ \tau_{C_4} + 3/2\ \tau_{M_6}
\end{aligned}$$

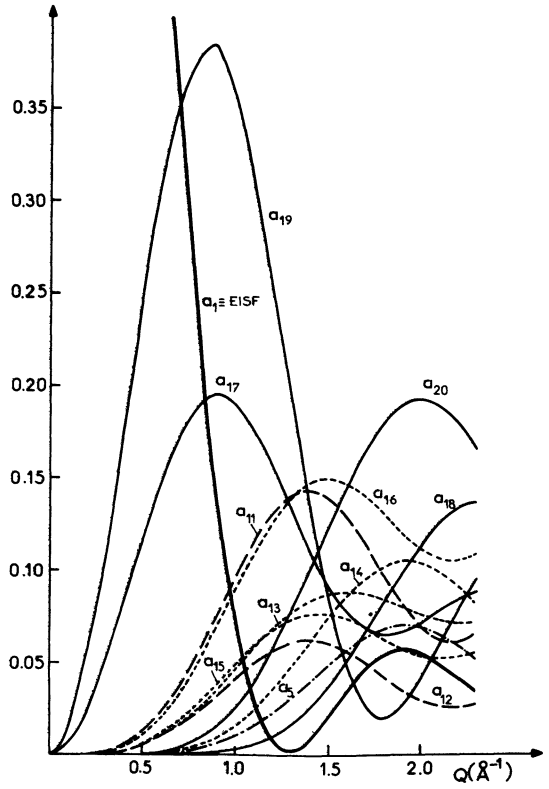

Fig. 6. — Elastic and quasielastic structure factors for the case of simultaneous rotations about molecular and crystalline axes (Eq. (19)).

general program ABUSEAM of the Laue-Langevin Institute library. The variation of the most significant terms as function of Q is shown in figure 6. Only twelve of them have significant values. For the multiple scattering evaluation (see below), some of them were assumed to be equal so as to reduce the number of terms in the evaluation of second and third order of scattering.

3. **Experimental set-up and data corrections.** — The experiments were performed at the Institute Laue-Langevin. Several sets of measurements were performed. In the first, the four-chopper time-of-flight spectrometer, IN5, was used with the energy of the incident neutrons being 1.004 meV (wavelength $\lambda = 9.026$ Å) corresponding to an energy resolution ranging from 0.023 to 0.027 meV (fwhm) depending on the angle of scattering. Spectra were recorded at 14 angles, simultaneously. Bicyclo-octane was studied at 8 temperatures in its plastic phase, at $T = 173$ K, 183 K, 213 K, 229 K, 257 K, 298 K, 328 K and 359 K. Another measurement was performed at $T = 150$ K in the low temperature phase just below the transition point. At the highest temperatures, an important quasielastic broadening was observed. Another set of experiments were performed using the time focusing time-of-flight spectrometer IN6. As well as improving the statistics (higher incoming neutron flux), the use of this instrument enabled spectra beyond the minimum in the EISF curve to be obtained with a better resolution than that of IN5. Two experiments were carried out with the sample at room temperature using incident neutron wavelength of 5.9 Å and 4.1 Å, to determine whether the use of different incident energies, i.e. of different instrument resolutions (fwhm 0.076 meV and 0.200 meV respectively) was amplifying some aspects of the scattering function. Measurements at $T = 323$ K, 383 K and 423 K were performed with an intermediate incident wavelength $\lambda = 5.1$ Å (fwhm 0.098 meV).

The powdered sample of bicyclo-octane (transmission : 0.92) was held in a slab-shaped container of circular geometry 0.3 × 50 mm in size, with thin walls of aluminium plates. The sample was maintained at room temperature and above, by placing the container in a sample holder, the temperature of which was regulated by adjusting the current passing through heating coils. For measurements below room temperature, the container was put into a liquid nitrogen cryostat. In both cases deviations in the temperature stability were less than one degree. In all the experiments performed on IN5 the angle between the plane of the sample and the incoming neutron beam was 45°. Using such a geometry, the angular range shadowed by the sides of the sample container was outside the minimum of the EISF (see Figs. 2, 6). For IN6 measurements, the sample was placed at an angle of 135° and all spectra were recorded in transmission geometry.

Using the standard correction programs IN5PDP and IN6PDP of the Institute Laue-Langevin library, the following corrections were applied to the measured time-of-flight spectra obtained at constant angle :

a) Normalization of the various sets of measured spectra to the incident neutron flux.

b) Normalization according to the efficiency of the neutron detector banks from the measurement of a vanadium standard.

c) Subtraction of background due to sample holder and container (evaluated from an empty container measurement).

d) Absorption and self shielding corrections.

The time-of-flight spectra were transformed to $S(\phi, \omega)$ at constant scattering angle ϕ. Data collected at the same temperature with the same value of incoming neutron energy were compared by a least-squares-fit to the following scattering function :

$$S_{\text{inc}}(Q, \omega) = e^{-2W} S^{\text{R}}_{\text{inc}}(Q, \omega) + S^{\text{M}}_{\text{inc}}(Q, \omega) + S^{\text{I}}_{\text{inc}}(Q, \omega) \tag{20}$$

folded with the instrument resolution. In this expression, $S^{\text{R}}_{\text{inc}}(Q, \omega)$ is the rotational scattering function which corresponds to the assumed model. The attenuation effect in the quasielastic region caused by periodic lattice motions was taken into account by the Debye-Waller factor e^{-2W}. $S^{\text{I}}_{\text{inc}}(Q, \omega)$ is an inelastic term which contributes only little to the scattering in the quasielastic region under the form of a slowly varying function of energy. It can be taken into account by a one-phonon expansion [16]. The multiple scattering contribution $S^{\text{M}}_{\text{inc}}(Q, \omega)$ can be evaluated from a semi-analytical calculation [18]. This involves multiple convolutions of the single scattering function with itself, taking into account the experimental geometry. Referring to figures 2 and 6 for the variation of the first-order structure factors as function of the momentum transfer Q, only the most significant contributions were used for this calculation. In fact, the thickness of the sample had been chosen as thin as possible in order to reduce these effects. They were evaluated to be less than 5 % of the total scattering. Readers are referred to reference [18] for more information.

4. **Results and discussion.** — 4.1 HIGH-TEMPERATURE PLASTIC PHASE TIME-OF-FLIGHT SPECTRA. — Some typical examples of time-of-flight spectra, with the sample at room temperature are shown in figure 7. The energy of incoming neutrons was 1.004 meV. The main feature is the strong quasielastic broadening, suggesting rapid motions of the protons. Moreover, the important decrease of the purely elastic peak with increasing the modulus of Q has to be interpreted as reflecting a great number of equilibrium positions accessible to each proton, and suggesting the existence of nearly isotropic reorientations at

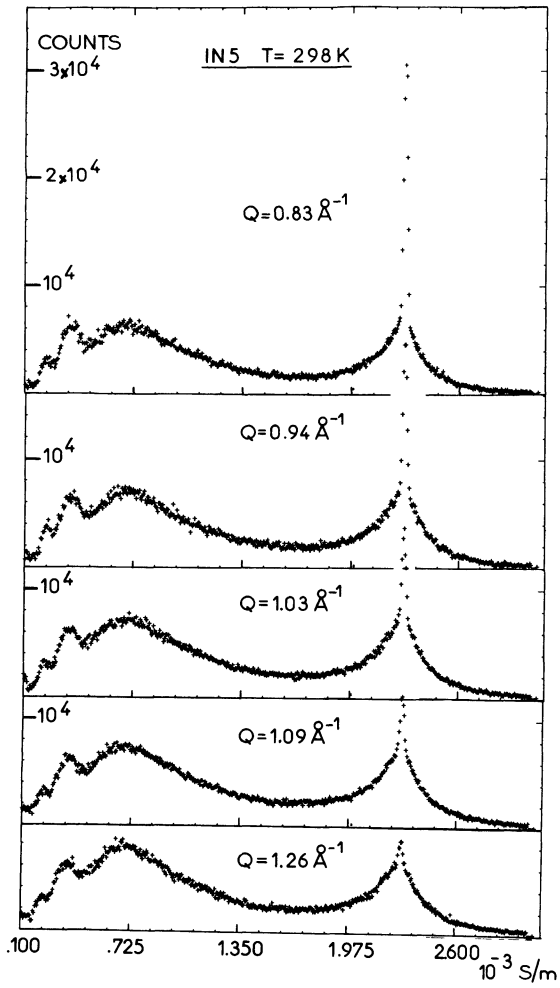

Fig. 7. — IN5 time-of-flight spectra obtained at 298 K (λ = 9.02 Å).

this temperature. We note also in the quasielastic region a significant contribution from the part of the spectra related to lattice vibrations. Thus the $S^{I}_{inc}(Q, \omega)$ term in (20) cannot be neglected.

4.2 Determination of the experimental EISF. — Usually an experimental EISF is determined after separation of the elastic and quasielastic parts of the spectra by natural extrapolation and then graphically integration. A more systematic method for the determination of the EISF from the experimental data uses a nonlinear least-squares fitting procedure. This latter method had already been used successfully in the case of a weak quasielastic broadening [16]. This was achieved by fitting to the data an expression with a weight parameter $f(Q)$ controlling the amount of elastic scattering. Separating the rotational scattering function $S^{R}_{inc}(Q, \omega)$ given by (2) or (5) into its elastic and quasielastic $\tilde{S}^{R}_{inc}(Q, \omega)$ parts :

$$S^{R}_{inc}(Q, \omega) = A_0(Q)\, \delta(\omega) + \tilde{S}^{R}_{inc}(Q, \omega) \qquad (21)$$

we define

$$S^{R}_{fit}(Q, \omega) = \left[f(Q)\, A_0(Q)\, \delta(\omega) + \frac{1 - f(Q)\, A_0(Q)}{1 - A_0(Q)}\, \tilde{S}^{R}_{inc}(Q, \omega) \right] \qquad (22a)$$

$$S_{fit}(Q, \omega) = e^{-2W}\, S^{R}_{fit}(Q, \omega) + S^{I}_{inc}(Q, \omega) \qquad (22b)$$

$S^{I}_{inc}(Q, \omega)$ is the inelastic term occurring in (20), while multiple scattering effects are assumed sufficiently weak to be taken into account by $f(Q)$.

In constructing $S^{R}_{fit}(Q, \omega)$, the following three constraints are observed :

1) Since the Lorentzian functions occurring in $\tilde{S}^{R}_{inc}(Q, \omega)$ are normalized to unity and according to the fact that the sum of all the elastic and quasielastic structure factors is equal to 1, the energy integral of $S^{R}_{fit}(Q, \omega)$ is equal to 1.

2) $S^{R}_{fit}(Q, \omega) = S^{R}_{inc}(Q, \omega)$ for $f(Q) = 1$.

3) If $f(Q)$ is set $\neq 1$, then only the ratio of elastic to quasielastic intensity is varied, whereas the shape of $\tilde{S}^{R}_{inc}(Q, \omega)$ remains unchanged.

The fit of a theoretical model which correctly describes the dynamics of the molecular motion, must result in $f(Q) = 1$ for all scattering angles. However, if $f(Q)$ deviates appreciably from 1, then the product $f(Q)\, A_0(Q)$ can nevertheless be expected to tend towards the real (experimental) EISF. Then a more realistic model may be selected. Figure 8 shows the evolution of the spectrum as a function of temperature corresponding to the wavevector transfer Q = 1.09 Å^{-1}, i.e. a value about the minimum in the EISF curves. At T = 298 K, the quasielastic peak is appreciably broadened. The purely elastic contribution is very small. From the EISF curves (Figs. 2 to 6) it is clear that reorientations about crystalline

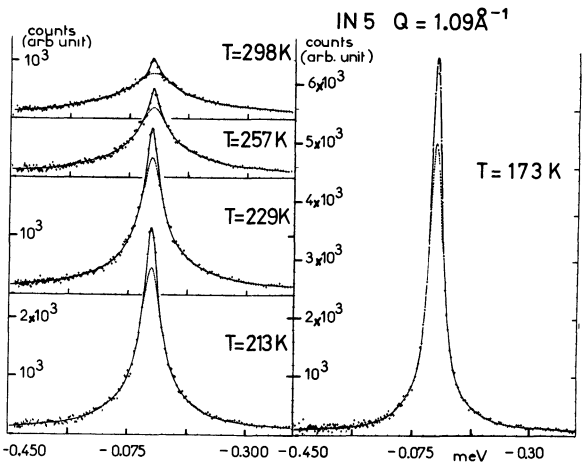

Fig. 8. — Temperature evolution of the IN5 energy spectrum at Q = 1.09 Å^{-1}. The full curve is the result of the fit of jump model allowing reorientations about both molecular and crystalline axes. The dashed line is the elastic separation obtained from refinement.

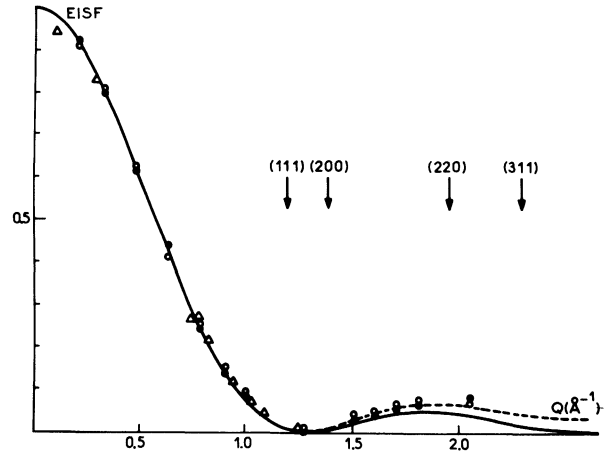

Fig. 9. — Determination of the experimental EISF at $T = 298$ K. Closed circles are $f(Q)\,A_0(Q)$ values obtained by fitting (22) based on the rotational diffusion model (IN6 $\lambda = 5.1$ Å). Results of fitting (22) based on the jump model allowing two kinds of motions are in open symbols (circles for IN6, triangles for IN5). Bragg peaks are indicated by arrows. The full (resp. dotted) curve corresponds to the theoretical EISF for the rotational diffusion (resp. jump) model.

axes are involved in the motion of the molecule. Uniaxial models can be discarded. Subsequently this result was confirmed by fitting (22) to the spectra, with $A_0(Q)$ and $\tilde{S}^{R}_{inc}(Q, \omega)$ based on the rotational diffusion model. The final values of the $f(Q)$ factor were larger than 1, yielding the experimental EISF $f(Q)\,A_0(Q)$ indicated on figure 9 by full circles. There is good agreement with the function $A_0(Q)$ for simultaneous jumps about molecular and crystalline axes. As a further test, another fit based on this jump model was made using (22). The results are indicated on figure 9 by open circles. The final values of the $f(Q)$ factors are again close to 1 for all values of Q. For $Q > 1$ Å^{-1}, these values are in both cases slightly above the theoretical curve. Such a deviation is characteristic of multiple scattering effects.

At lower temperature, the spectrum exhibits the shape of a sharp peak, with a small quasielastic broadening. The purely elastic contribution is not easily separated from the whole scattering and it is difficult to determine by simple visualization if the shape of the measured spectra can be described by using one or both kinds of motion. A fit of (22) to the spectra was made, based on the uniaxial jump model (5). The resulting $f(Q)$ values were much smaller than 1, and thus the product $f(Q).A_0(Q)$ again tended towards the EISF corresponding the two motions, even at $T = 173$ K.

4.3 Fit of various dynamical models. — At higher sample temperatures, refinements of (22) based on the rotational diffusion equation led to the same conclusion as for samples at room temperature. However, final values of $f(Q)$ do not differ greatly from 1. In the jump model picture, 48 equilibrium positions are accessible to each individual proton on a sphere. Large molecular librations together with reorientational jumps allow the proton to access all the points of the sphere as the temperature is increased. Clearly, points in the vicinity of the equilibrium position are more likely to be occupied. Then it is interesting to test the validity of this model. The rotational constant D_R is the only adjustable parameter and its fitted value must be independent of the wavevector transfer. Subsequently spectra recorded at different scattering angles were fitted separately.

In order to have a rigorous treatment, the multiple scattering terms $S^{M}_{inc}(Q, \omega)$ occurring in (20) was taken into account up to third scattering assuming a scattering law with $l \leqslant 4$ (see Eq. (2)) for second order and $l \leqslant 3$ for third order (refer to Fig. 2 for evaluation of the importance of different terms).

Good fits were obtained for the highest temperatures. Refinements of IN5 and IN6 spectra led to a small Q dependence of D_R, as indicated on figure 10, but at lower temperature, the final values of D_R were strongly varying with Q. Moreover, simultaneous refinements of all spectra recorded at the same temperature led to real discrepancies not only in the magnitude of purely elastic scattering but also in the shape of the spectra, so that this model could be ruled out at these temperatures. In IN6 experiments, wavevector transfers up to $Q \simeq 2.5$ Å^{-1} ($\lambda = 4.1$ Å) could be accessed, and in principle differences between the jump model and the continuous model would be enhanced, even for the highest temperatures (Figs. 2 and 3). However the instrumental resolution is inferior to that at high Q and the elastic and quasielastic parts of the spectra are less-well separated. In fact, when the temperature is increased, both models become less valid. In particular time-of-flight spectra show a coupling between translational and rotational

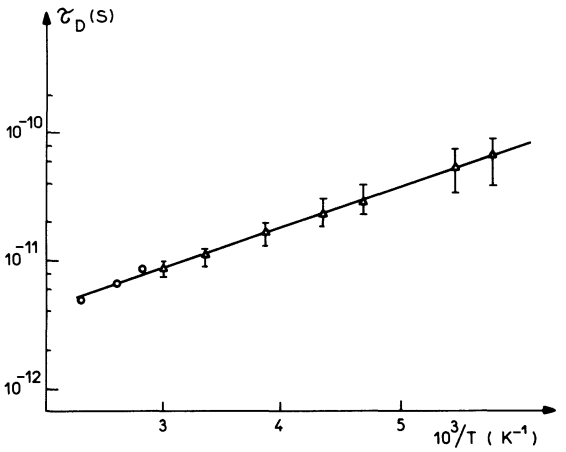

Fig. 10. — Isotropic rotational diffusion correlation time $\tau_D = 1/D_R$ as function of temperature. Results of fit of individual IN5 spectra determine the error bar. Triangles correspond to a fit of all spectra simultaneously. Circles are IN6 results.

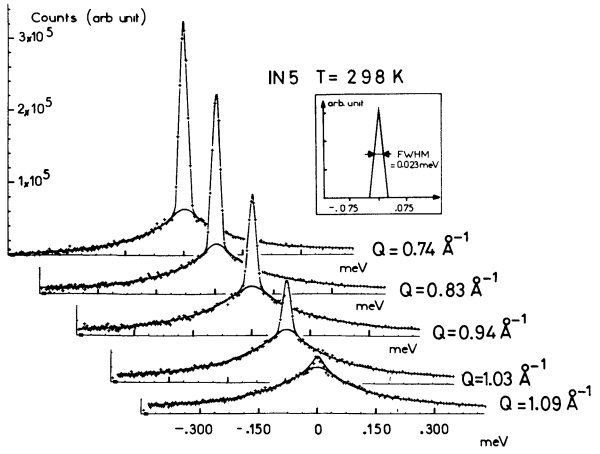

Fig. 11. — Comparison of experimental IN5 energy spectra with the jump model allowing two kinds of reorientations.

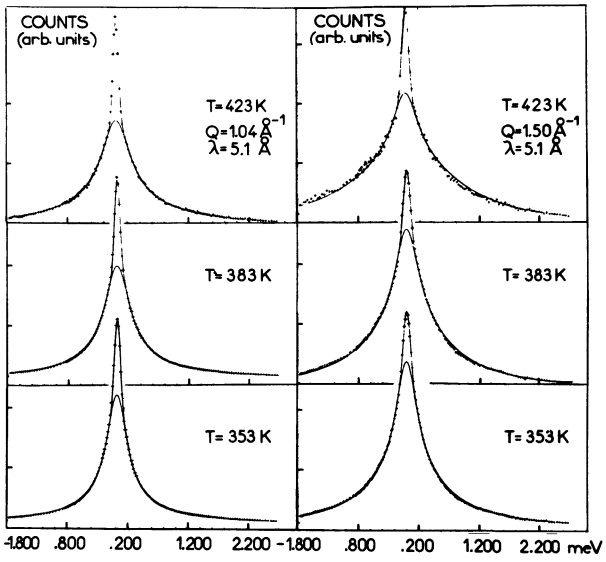

Fig. 12. — Temperature evolution of IN6 energy spectra. The full curve is the result of the fit of the jump model.

motions (the separation between the inelastic and quasielastic part of the spectra is not well-defined). As we are mainly interested in the motions up to and slightly above room temperature, the framework of the jump model is retained.

All spectra recorded at the same temperature, using the same incident energy were fitted simultaneously, assuming M_6 rotations about the molecular axis together with C_4 rotations around [100] lattice directions. Only the non-negligible terms given by (19) were taken into account. Moreover, for the multiple scattering evaluation, the following assumptions were made in order to reduce the number of relevant terms (see Fig. 6).

For second order :

$$\begin{aligned} a_5(Q) &\simeq a_{14}(Q) \\ a_{11}(Q) &\simeq a_{16}(Q) \\ a_{12}(Q) &\simeq a_{13}(Q) \simeq a_{15}(Q) . \end{aligned} \tag{23a}$$

For third order

$$\begin{aligned} a_5(Q) &\simeq a_{12}(Q) \simeq a_{14}(Q) \simeq a_{15}(Q) \\ a_{11}(Q) &\simeq a_{16}(Q) \\ a_{18}(Q) &\simeq a_{20}(Q) . \end{aligned} \tag{23b}$$

Then we had, respectively, 12, 8×8 and $6 \times 6 \times 6$ terms in the expansion of first, second and third scattering [18].

Good fits were obtained at each temperature for all the energies of incoming neutrons (see Figs. 8 and 12). At the two lowest temperatures $T = 183$ K and $T = 173$ K, the fits led to values of the jump probability $1/\tau_{C_4}$ around the lattice axes near the limit of the IN5 range ($\tau_{C_4}^{-1} = 1.4 \times 10^{10}\ s^{-1}$ and $10^{11}\ s^{-1}$, respectively). However, a fit on the basis of (5) i.e. taking into account the uniaxial rotational 60° jumps could not correctly describe the observed spectra. At the highest temperatures, both IN5 and IN6 measurements led to the same values of the correlation times (Fig. 13). In fact, IN6 resolution at $\lambda = 5.1$ Å is sufficient to analyse accurately both motions at $T = 323$, 383 or 423 K. Resolution is strongly angle-dependent (fwhm : from 0.070 to 0.130 meV). However, it can be seen from figure 6 that the quasielastic structure factors which are predominant at small Q values are $a_{17}(Q)$ and $a_{19}(Q)$. The former is related to the motion about the crystalline axes alone, i.e. the slowest that can then be determined accurately, taking advantage of the better instrument resolution. Structure factors related to the molecular axial rotation (e.g. $a_{16}(Q)$, $a_{18}(Q)$, $a_{20}(Q)$, etc.) mainly contribute at large Q value. These are related to the wider Lorentzian functions and

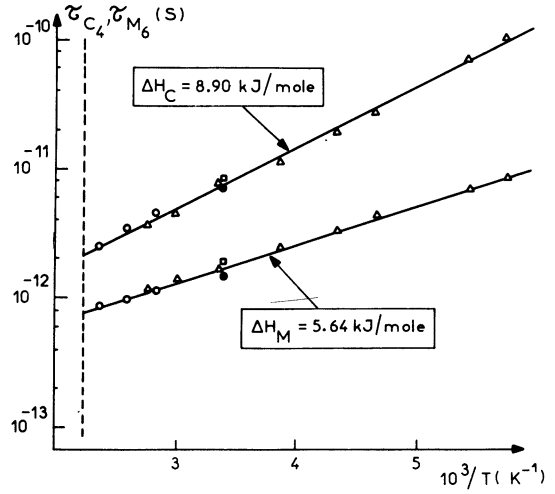

Fig. 13. — Correlation times for the two motions of bicyclo [2, 2, 2] octane; triangles : IN5 results, open circles : IN6 $\lambda = 5.1$ Å, closed circles : IN6 $\lambda = 4.1$ Å, squares : IN6 $\lambda = 5.9$ Å.

instrument resolution is not as critical for their determination.

For these reasons, even at room temperature, measurements with $\lambda = 4.1$ Å enable us to obtain correlation time values in reasonable agreement with those obtained from IN5 measurements.

Figure 13 shows the variation of the two correlation times as a function of temperature. Two straight lines can be drawn across the experimental points. They correspond to the Arrhénius laws :

$$\tau_{C_4} = 1.952 \times 10^{-13} \exp(\Delta H_C/RT) \text{ s} \quad (24a)$$

$$\tau_{M_6} = 1.743 \times 10^{-13} \exp(\Delta H_M/RT) \text{ s} \quad (24b)$$

with the two activation energies

$\Delta H_C = 8.90$ kJ/mole for the crystalline reorientations,

$\Delta H_M = 5.64$ kJ/mole for the axial rotations, respectively.

4.4 LOW-TEMPERATURE PHASE. — Figure 14 illustrates that no quasielastic broadening is visible in the low temperature phase ($T = 150$ K, $\lambda = 9.02$ Å). Investigation of possible motions in this phase (between indistinguishable equilibrium positions) would require a much better resolution than that of IN5.

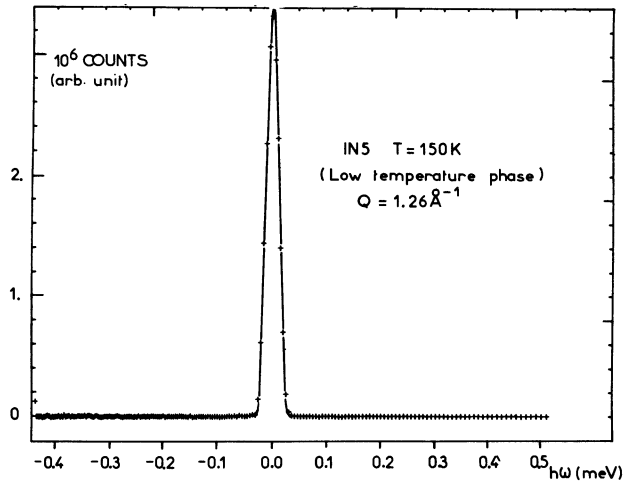

Fig. 14. — IN5 spectrum for low temperature phase of bicyclo [2, 2, 2] octane.

5. **Summary.** — From quasielastic neutron scattering performed in the two crystalline phases of bicyclo [2, 2, 2] octane, detailed information about the dynamical behaviour of the molecule was obtained. In the low-temperature phase no quasielastic broadening was observed in the energy spectra, but above 173 K, the time-of-flight spectra indicated the occurrence of fast reorientations. Both IN5 and IN6 measurements were in agreement with a model of 60° jumps of the molecule about its symmetry axis together with 90° jumps of the molecule around crystallographic [100] directions. The basic assumption throughout this paper was the absence of correlation between different motions. This hypothesis was certainly less valid when the temperature was increased. Indeed we have shown that at the highest temperatures of the experiment, the observed spectra could be described on the basis of an isotropic diffusion model. Brot *et al.* [7] have investigated the plastic phase of quinuclidine at room temperature. They found that the isotropic rotational diffusion model was excluded, and that the situation which was more likely to be valid was described by a model allowing for 90° jumps about crystallographic [100] axes and 120° reorientations about the molecular axis. This model yields to the corresponding correlation times

$$\tau_{C_4} = 22.5 \times 10^{-12} \text{ s}$$

$$\tau_{M_3} = 8.7 \times 10^{-12} \text{ s}.$$

We can conclude that molecular motions are very similar in these both compounds. However, the disorder in bicyclo-octane is somewhat greater. First, the reorientations about the molecular axis occur between distinguishable positions and second the residence times are shorter. Indeed according to (24) we obtain at $T = 298$ K

$$\tau_{C_4} = 7.1 \times 10^{-12} \text{ s}$$

$$\tau_{M_6} = 1.7 \times 10^{-12} \text{ s}.$$

A comparison of the height of the rotational energy barriers would be fruitful. Unfortunately, quinuclidine was studied at room temperature only.

As we have already mentioned, we have also investigated both the low- and the high-temperature phases of the third similar compound, triethylediamine. Results will be reported elsewhere.

Acknowledgments. — We would like to thank S. Jenkins, Y. Blanc, A. J. Dianoux and F. Douchin for technical assistance during the experiments. We are indebted to C. Carpentier and M. Muller for purifying the compound and to Dr. J. P. Beaufils for critically reading the manuscript. We are also obliged to Prof. R. Fouret for his constant interest for this work.

References

[1] HULLER, A., *Faraday Discuss. Chem. Soc.* **69** (1980) 66.

[2] WEN-KUEI WONG, WESTRUM Jr., E. F., *J. Phys. Chem.* **74** (1970) 6.

[3] BRUESH, P., *Spectrochim. Acta* **22** (1966) 861.

[4] SAUVAJOL, J. L. and AMOUREUX, J. P., *J. Phys. C* **14** (1981) 1537.

[5] FOURME, R., *J. Physique* **40** (1979) 557.
[6] BROT, C. and VIRLET, J., *J. Physique* **40** (1979) 573.
[7] BROT, C., LASSIER-GOVERS, B., LECHNER, R. E. and VOLINO, F., *J. Physique* **40** (1979) 563.
[8] SEARS, V. F., *Can. J. Phys.* **44** (1966) 1299, *ibidem* **45** (1967) 234.
[9] FRENKEL, J., *Acta Phys. Chem. USSR* **3** (1935) 23.
[10] DIANOUX, A. J., VOLINO F. and HERVET. H., *Mol. Phys.* **30** (1975) 1181.
[11] HERVET, H., VOLINO, F., DIANOUX, A. J. and LECHNER, R. E., *J. Physique-Lett.* **35** (1974) L-151.
[12] RIGNY, P., *Physica* **59** (1972) 707.
[13] THIBAUDIER, C. and VOLINO, F., *Mol. Phys.* **26,** 5 (1973) 1281.
[14] THIBAUDIER, C. and VOLINO, F., *Mol. Phys.* **30,** 4 (1975) 1159.
[15] LEADBETTER, A. J. and LECHNER, R. E., *The Plastically Crystalline State*, edited by J. N. Sherwood (John Wiley & Sons) 1979.
[16] LECHNER, R. E., AMOUREUX, J. P., BÉE, M. and FOURET, R., *Commun. Phys.* **2** (1977).
[17] BÉE, M., Thesis University of Lille I (1980).
[18] BÉE, M. and AMOUREUX, J. P., *Mol. Phys.* **41,** 2 (1980) 287.
[19] AMOUREUX, J. P., SAUVAJOL, J. L. and BÉE, M., *Acta Crystallogr.* **A 37** (1981) 97.